Published in final edited form as:
Eur J Nucl Med Mol Imaging. 2011 September ; 38(9): 1723–1731. doi:10.1007/s00259-011-1831-z.

The potential use of 2-[^{18}F]fluoro-2-deoxy-$_D$-galactose as a PET/CT tracer for detection of hepatocellular carcinoma

Michael Sørensen[1,2], **Kim Frisch**[1], **Dirk Bender**[1], and **Susanne Keiding**[1,2]

[1]PET Centre, Aarhus University Hospital, Aarhus, Denmark

[2]Department of Medicine V (Hepatology and Gastroenterology), Aarhus University Hospital, Aarhus, Denmark

Abstract

Purpose—To evaluate the feasibility of using the hepatocyte specific PET tracer 2-[^{18}F]fluoro-2-deoxy-$_D$-galactose (FDGal) as a tracer for hepatocellular carcinoma (HCC).

Methods—In addition to standard clinical investigations, 39 patients with known HCC or suspected to have HCC underwent a part-body FDGal PET/CT (from base of skull to mid-thigh). Diagnosis of HCC was based on internationally approved criteria. FDGal PET/CT images were analyzed for areas with high (*hot spots*) or low (*cold spots*) tracer accumulation when compared to surrounding tissue.

Results—Seven patients did not have HCC and FDGal PET/CT was negative in each of them. Twenty-three patients had HCC and were included before treatment; FDGal PET/CT correctly identified 22 of these patients, which was comparable to contrast-enhanced CT. Interestingly, FDGal PET/CT was conclusive in 12 patients in whom conventional imaging techniques were inconclusive and required additional diagnostic investigations or close follow-up. Nine patients were included after treatment of HCC and in these patients FDGal PET/CT was able to distinguish between viable tumour tissue as *hot spots* and areas with low metabolic activity as *cold spots*. FDGal PET/CT detected extra-hepatic disease in nine patients which was a novel finding in eight patients.

Conclusion—FDGal PET/CT has great clinical potential as a PET tracer for detection of extra- but also intra-hepatic HCC. In the present study, the specificity of FDGal PET/CT was 100%, which is very promising but needs to be confirmed in a larger, prospective study.

Keywords

Nuclear hepatology; Cirrhosis; Hepatobiliary cancer; Molecular imaging; FDGal

Introduction

Hepatocellular carcinoma (HCC) is a primary liver cancer derived from hepatocytes. Worldwide, HCC is the sixth most common cancer and the third cause of cancer-related death [1]. Liver cirrhosis significantly increases the lifetime risk of developing HCC and in more than 80 percent of the cases HCC develops in association with liver cirrhosis [2]. Advances in treatment of cirrhosis have improved the survival of these patients and HCC is now the leading cause of death in patients with cirrhosis [2]. HCC is potentially curable by

Corresponding author Michael Sørensen, PET Centre, Aarhus University Hospital, DK-8000 Aarhus C, Denmark, michael@pet.auh.dk, Homepage: http://www.liver.dk.

Conflicts of interest None.

liver transplantation, resection or radiofrequency ablation (RFA) [3] and the goal of surveillance programs is to detect HCC at an early stage defined as a lesion with a diameter <20 mm [3–6]. For this purpose, guidelines proposing diagnostic algorithms for optimized clinical management of the patient with an increased risk of developing HCC have been published [5, 6]. These guidelines are primarily based on radiological examinations such as contrast-enhanced ultrasound sonography (US), multi-phase computer-assisted tomography (CT) and magnetic resonance imaging (MRI) [2–11] but for small HCC the sensitivity of the noninvasive criteria is only around 30% [4]. Biopsy is the gold standard, but may be difficult to obtain from small liver lesions as small lesions are difficult to target with the biopsy needle or simply cannot be visualized with US used to guide the needle [12]; for small HCC lesions, a false negative rate of 30% has been reported for the first fine-needle biopsy [4]. Moreover, risks are related to the invasive biopsy procedure and the development of improved noninvasive diagnostic tools is therefore of utmost importance for better diagnosis of HCC.

Positron emission tomography (PET) with the glucose analogue 2-[^{18}F]fluoro-2-deoxy-$_D$-glucose, FDG, is widely used in oncology, but FDG PET misses 30–50% of HCC lesions [13–16]. The feasibility of using PET tracers of other metabolic pathways have been published, most recently [^{11}C]-labelled acetate [17–21], [^{18}F]-labelled choline [22], [^{11}C]-labelled choline [23], and [^{18}F]-labelled fluorothymidine [24], but so far no studies have been convincing when using the tracers as single molecular imaging modalities. The largest prospective study with comparison of ^{11}C-acetate and FDG PET/CT concluded that both ^{11}C-acetate and FDG PET/CT as well as the two tracers used in combination had low sensitivity for the detection of small primary HCC [20]. Accordingly there is still a need for better imaging modalities for detection of HCC. A couple of decades ago, a few promising PET studies using the galactose analogue 2-[^{18}F]fluoro-2-deoxy-$_D$-galactose (FDGal) in experimental tumour models were published [25–28] but to the best of our knowledge no FDGal PET studies of patients with HCC have been published. FDGal is a tracer for galactose metabolism and avidly accumulates in the liver compared to other tissues [29–30]. FDGal can be synthesized using commercially available kits for FDG production with only minor modifications [31] and the production can thus readily be implemented at most clinical PET facilities or distributed to other nearby centres due to the radioactive half-life of 110 minutes. In the present feasibility study, we tested the potential use of FDGal as a PET tracer for HCC in patients with or suspected to have HCC. The aim was to study the uptake pattern of FDGal in intra- and extra-hepatic HCC lesions.

Materials and methods

Patients

Thirty-nine patients were enrolled. The diagnosis of HCC was based on multiphase contrast-enhanced CT (ceCT) or MRI, plasma alpha-fetoprotein (AFP), contrast enhanced US, and/or histopathology according to internationally approved guidelines at the time of the study [5, 6]. All investigations were performed as *state-of-the-art*. Biopsy material was obtained from 29 patients. One patient (ID32) had a false-negative biopsy.

The study was approved by the Central Denmark Region Committees on Biomedical Research Ethics and conducted in accordance with the Helsinki II Declaration. The average radiation dose received from the FDGal PET/CT investigation was 4.4 mSv (range 2.0–8.9). No complications to the procedures were observed.

FDGal PET/CT

The patient fasted for at least six hours before the study but was encouraged to drink water. FDGal was produced according to a previously described procedure [31]. A part-body PET/CT recording from base of the skull to mid-thighs was performed 70–95 minutes after intravenous injection of FDGal in an antecubital vein (median radioactive dose was 100 MBq, range 60–262 MBq). The camera was a combined 40-slice Siemens Biograph TruePoint PET/CT camera (Siemens AG, Erlangen, Germany) with a transaxial field-of-view of 21 cm (5–7 bed positions, 3-min scan in each bed position). The CT-scan was a low-dose CT (120 kV; mAs according to body weight: 25 mAs if ≤ 70 kg, 30 mAs if 70–100 kg, and 50 mAs if ≥ 100 kg) and was reconstructed using a smooth filter and a slice thickness of 5 mm with an increment of 3 mm. PET data were reconstructed in an iterative mode using a Gaussian filter (8 mm full-width at half maximum) and the CT scan for attenuation correction yielding images with a central spatial resolution of 9 mm. Standardized uptake values (SUV) of FDGal were calculated by normalising the tissue concentrations of radioactivity for injected dose and body weight.

As FDGal is a novel PET tracer for human studies, we did not know the minimal tracer dose needed to achieve high-quality PET images when we initiated the study. Because the effective dose of FDGal is about twice that of FDG [31], we decided to start with a dose of 200 MBq which is half the dose normally used in FDG studies. Due to technical problems with the production of FDGal we injected 60 MBq in one patient (ID10). The quality of the PET images from this study was good and we accordingly decided to use a dose of 100 MBq FDGal in the subsequent patients.

Image interpretation

All FDGal PET/CT images were analyzed without knowledge of the clinical history of the patient and results from other imaging techniques and/or histopathology. The images were evaluated for lesions with increased or decreased uptake of FDGal compared to surrounding tissue. For an area with an increased uptake (*hot spot*) a tumour-to-background ratio (T/B-ratio) was defined as the maximum SUV in that area divided by the average SUV in surrounding tissue. A T/B-ratio for areas with low uptake (*cold spots*) were similarly noted as the minimum SUV in that area divided by the average SUV in surrounding tissue. The FDGal PET images were then analyzed again by viewing them side-by-side with the ceCT images and/or images from other imaging modalities and with knowledge of clinical information on the patient in order to decide whether the suspicious areas on the PET images corresponded to the suspicious areas on ceCT and *vice versa*. Because FDGal PET is a novel imaging technique, the first 15 cases were used to build experience and these cases were therefore reviewed again blinded for patient ID.

Results

39 patients were enrolled in the study; patient characteristics are given in Table 1. Twenty-three patients had HCC and had the FDGal PET/CT performed before receiving any treatment of the disease (Table 2). Nine subjects were included after previous treatment for HCC (Table 3). Seven patients were suspected to have HCC, but did not (Table 4).

As seen in Table 1, alcohol (n=12) and viral hepatitis C (n=10) were dominant etiological factors. The majority of patients with liver disease were stable being in Child-Pugh [32] class A (n=19), 9 patients were in class B, and only 4 patient were in class C. Seven patients were not classified according to the Child-Pugh score because they did not have any underlying liver disease.

Patients with HCC included before treatment

Of the 23 patients with HCC investigated before receiving any treatment, seven patients had one or few FDGal positive nodules with T/B-ratios between 1.2–1.9, i.e. *hot spots* (Table 2). For all seven patients, the FDGal PET/CT was in accordance with other imaging modalities and clinical information. Fig. 1 shows an example of a single nodule in the right liver lobe of a patient (ID33) with severe cirrhosis. ID22 had one large tumour with central necrosis; the T/B-ratio was 1.5 in the viable tumour tissue and 0.4 in the necrotic area (Fig. 2). In ID27, FDGal PET/CT showed three lesions with SUV values between 1.4 and 1.8 whereas ceCT showed no lesions and MRI showed one lesion; a biopsy showed HCC and follow-up showed rapid progression with several lesions on US and the patient died 46 days later. In ID06, FDGal PET/CT showed more suspicious areas than ceCT and follow-up showed progression in these areas.

In ten cases (Table 2), the FDGal PET/CT images were interpreted as multinodular disease with an average T/B-ratio of 1.6 (1.3–2.8). In all ten cases, the areas of increased FDGal uptake corresponded with areas identified as tumour nodules on ceCT. In ID19, areas of necrotic tumour tissue were scattered within the large multinodular tumour. In ID20, other imaging modalities did not suggest multinodular disease at the time that FDGal PET/CT was performed, but close follow-up showed rapid progression to multinodular disease.

In five cases, the FDGal PET/CT images revealed only areas of low FDGal uptake when compared to the surrounding liver tissue (mean T/B-ratio 0.5, range 0.2–0.8). This corresponded to tumours being described as necrotic and/or hypoperfused on ceCT. FDGal PET/CT was thus able to detect tumour areas with low metabolic activity as *cold spots*. Fig. 3 shows an example of a tumour with low metabolic activity.

In one case (In ID28), FDGal PET/CT was false-negative, as it did not reveal any *hot* or *cold spots*, whereas both ceCT and US showed a lesion. The HCC diagnosis was confirmed by a biopsy.

Patients included after treatment of HCC

The results from the nine patients with suspected relapse after previous treatment of HCC are summarized in Table 3. In all nine cases, FDGal PET/CT was in accordance with other imaging modalities and clinical information. In ID39, pre-treatment ceCT showed several lesions and a series of transarterial chemoembolization (TACE) was planned. FDGal PET/CT was performed after the first series and showed low uptake in the treated area (*cold spot*) and high uptake (*hot spot*) in the area still to be treated.

ID34 had previously been treated for HCC and relapse was suspected due to the finding of a tumour mass in the left kidney on MRI. FDGal PET/CT was without any suspicious lesions in the liver and the tumour mass in the kidney did not accumulate FDGal. A biopsy showed renal cell carcinoma and the patient accordingly did not have relapse of the HCC but had developed a second cancer.

Patients without HCC

FDGal PET/CT was without any *hot* or *cold spots* in all seven cases suspected to have HCC but in whom the diagnosis was refuted (Table 4). In all cases, plasma AFP was normal (1–46 ng/ml) and ceCT showed suspicious but inconclusive lesions and enhanced follow-up was necessary to reach a final diagnosis.

Extra-hepatic disease

Nine of the patients had extra-hepatic metastases which were FDGal PET/CT positive (Table 5). While the presence of extra-hepatic disease was known in ID13, it was a novel finding in the other eight cases. Fig. 4 shows an example of an extra-hepatic metastasis in the neck of the left femur bone.

Discussion

This paper presents the first clinical study of the potential use of FDGal PET/CT for the detection of HCC. The main results are the ability of FDGal PET/CT to detect extra-hepatic HCC lesions and the interesting fact that FDGal PET/CT was negative in all patients in whom HCC was suspected but the diagnosis refuted. Furthermore, FDGal PET/CT could visualise metabolically active intra-hepatic HCC lesions with a T/B-ratio between 1.2 and 2.8. In patients with tumours described as being necrotic or hypoperfused on other imaging modalities, the T/B-ratio of FDGal was between 0.2 and 0.8 which indicates low metabolic activity. Evaluated on a patient-to-patient basis, FDGal PET/CT was true-positive in 22 out of the 23 patients with HCC who were included before treatment. This was comparable to multi-phase ceCT, which was also true-positive in 22/23 and is used as *state-of-the-art* imaging modality for radiological diagnosis of HCC at many centres. Interestingly, the two imaging modalities did not miss the same patient and in combination, they correctly identified all 23 patients.

In several cases, FDGal PET/CT showed definite *hot spots* in cases where ceCT was described as showing “suspicious areas” with the need for enhanced follow-up (Tables 2–4). In four cases (IDs 6, 20, 24, and 27), FDGal PET/CT detected more nodules than other imaging modalities at the time of investigation and follow-up showed rapid progression, indicating that FDGal PET/CT may be able to detect more lesions at an earlier time point than the conventional morphologically based imaging modalities. Due to the well-documented low sensitivity of FDG PET/CT for the detection of HCC [13–16], this imaging modality is not used as a standard clinical investigation of patients with HCC at our institution. Because of this we did not consider it useful to compare FDGal PET/CT with FDG PET/CT but instead preferred to compare FDGal PET/CT with standard clinical investigations. In the patients included after treatment of HCC (Table 3), FDGal PET/CT correctly identified subjects with relapse. This promising finding suggests that FDGal PET/CT may also be useful in monitoring treatment response in patients with HCC, but this needs to be tested in a larger, prospective clinical study.

FDGal PET/CT was true-negative in all seven patients without HCC. This indicates a high specificity of FDGal PET which is particularly interesting finding since CT, US and/or MRI were inconclusive in all seven cases, making enhanced follow-up necessary in order to reach a final diagnosis (Table 4). Actually, in ID40 ceCT, MRI and ultrasound showed a suspicious nodule which was negative on FDGal PET/CT and a biopsy showed that it was an adenoma. Although our material is too limited to draw any robust conclusion on the general specificity of FDGal PET/CT, we find the data encouraging. Moreover, the absence of false-positive lesions on the FDGal PET/CT images is interesting with regards to common benign and pre-malignant changes in cirrhotic livers such as the presence of regeneration and dysplastic nodules, which complicates the radiologic diagnosis of HCC [7, 8] and could be a potential source for false-positive FDGal PET/CT. However, our material indicates that FDGal does not accumulate in such nodules and a negative FDGal PET/CT thus seems to be a powerful supplement in ruling out HCC in patients with suspected HCC.

In eight of the nine cases with extra-hepatic disease, the presence of extra-hepatic disease was unknown prior to the FDGal PET/CT (Table 5). ID15 had an extra-hepatic metastasis in

a lymph node in the common hepato-biliary ligament, which was positive on FDGal PET/CT. Enlarged lymph nodes located in the common hepato-biliary ligament are often seen in patients with cirrhosis and using conventional imaging techniques it may be difficult to evaluate whether they are benign or malignant. The maximum SUV on FDGal PET/CT was 5, which was significantly higher than the surrounding tissue creating a T/B-ratio of 2.4. The metastasis was accordingly easily identified and the use of FDGal PET in conjunction with ceCT may increase the specificity of ceCT suspicious lymph nodes in that particular area.

Conclusion

Based on the present study, we believe that FDGal PET/CT is a promising imaging modality for detection of HCC. In particular, we find the apparently high specificity of FDGal PET/CT and the ability of the method to detect extra-hepatic HCC nodules interesting. The present study was a feasibility study and the clinical impact of FDGal PET/CT needs to be validated in a prospective clinical study. A key issue that needs to be studied is the potential use of FDGal PET/CT for detecting small intra-hepatic HCC lesions which are poorly visualized by existing imaging methods.

Acknowledgments

The authors are thankful to the patients included in the study and the staff at the PET Centre, the clinical teams at Dept. of Medicine V and the Liver Tumour Board at Aarhus University Hospital. The study was supported by grants from the Danish Medical Research Council (09-061564; 09-073658), the NIH (R01-DK074419) and the Danish Cancer Society (DP08024; DP06114).

References

1. Parkin DM, Bray F, Ferlay J, Pisani P. Global cancer statistics 2002. CA Cancer J Clin. 2005; 55:74–108. [PubMed: 15761078]
2. Llovet JM, Burroughs A, Bruix J. Hepatocellular carcinoma. Lancet. 2003; 362:1907–1917. [PubMed: 14667750]
3. Llovet JM, Bruix J. Novel advancements in the management of hepatocellular carcinoma in 2008. J Hepatol. 2008; 48:S20–S37. [PubMed: 18304676]
4. Forner A, Vilana R, Ayuso C, Bianchi L, Solé M, Ayuso JR, et al. Diagnosis of hepatic nodules 20 mm or smaller in cirrhosis: prospective validation of the noninvasive diagnostic criteria for hepatocellular Carcinoma. Hepatology. 2007; 47:97–104. [PubMed: 18069697]
5. Bruix J, Sherman M, Llovet JM, Beaugrand M, Lencioni R, Burroughs AK, et al. Clinical management of hepatocellular carcinoma. Conclusions of the Barcelona-2000 EASL conference. J Hepatol. 2001; 35:421–430. [PubMed: 11592607]
6. Bruix J, Sherman M. Management of hepatocellular carcinoma. Hepatology. 2005; 42:1208–1236. [PubMed: 16250051]
7. Lim JH, Kim EY, Lee WJ, Lim HK, Do YS, Choo IW, et al. Regenerative nodules in liver cirrhosis: findings at CT during arterial portography and CT hepatic arteriography with histopathologic correlation. Radiology. 1999; 210:451–458. [PubMed: 10207429]
8. Matsui O, Kadoya M, Kameyama T, Yoshikawa J, Takashima T, Nakanuma Y, et al. Benign and malignant nodules in cirrhotic livers: distinction based on blood supply. Radiology. 1991; 178:493–497. [PubMed: 1846240]
9. Brancatelli G, Federle MP, Ambrosini R, Lagalla R, Carriero A, Midiri M, et al. Cirrhosis: CT and MR imaging evaluation. Eur J Rad. 2007; 61:57–69.
10. Valls C, Cos M, Figuera J, Andía E, Ramos E, Sánchez A, et al. Pretransplantation diagnosis and taging of hepatocellular carcinoma in patients with cirrhosis: value of dual-phase helical CT. Am J Roentgenol. 2004; 182:1011–1017. [PubMed: 15039179]
11. Willat JH, Hussain HK, Adusumilli S, Marrero JA. MR imaging of hepatocellular carcinoma in the cirrhotic liver: challenges and controversies. Radiology. 2008; 247:311–330. [PubMed: 18430871]

12. Piscaglia F, Bolondi L. Recent advances in the diagnosis of hepatocellular carcinoma. Hepatol Res. 2007; 37 Suppl.2:S178–S192. [PubMed: 17877481]
13. Delbeke D, Martin WH. Update of PET and PET/CT for hepatobiliary and pancreatic malignancies. HPB. 2005; 7:166–179. [PubMed: 18333185]
14. Khan MA, Combs CS, Brunt EM, Lowe VJ, Wolverson MK, Solomon H, et al. Positron emission tomography scanning in the evaluation of hepatocellular carcinoma. J Hepatol. 2000; 32:792–797. [PubMed: 10845666]
15. Wudel LJ Jr, Delbeke D, Morris D, Rice M, Washington MK, Shyr Y, et al. The Role of [^{18}F]Fluorodeoxyglucose positron emission tomography imaging in the evaluation of hepatocellular carcinoma. Am Surg. 2003; 69:117–126. [PubMed: 12641351]
16. Sugiyama M, Sakahara H, Torizuka T, Kanno T, Nakamura F, Futatsubashi M, et al. ^{18}F-FDG PET in the detection of extrahepatic metastases from hepatocellular carcinoma. J Gastroenterol. 2004; 39:961–968. [PubMed: 15549449]
17. Ho CL, Yu SCH, Yeung DWC. ^{11}C-Acetate PET Imaging in hepatocellular carcinoma and other liver masses. J Nucl Med. 2003; 44:213–221. [PubMed: 12571212]
18. Li S, Beheshti M, Peck-Radosavljevic M, Oezer S, Grumbeck E, Schmid M, et al. Comparison of ^{11}C-acetate positron emission tomography and ^{67}Gallium citrate scintigraphy in patients with hepatocellular carcinoma. Liver Int. 2006; 26:920–927. [PubMed: 16953831]
19. Ho C, Chen S, Yeung DWC, Cheng TKC. Dual-tracer PET/CT imaging in evaluation of metastatic hepatocellular carcinoma. J Nucl Med. 2007; 48:902–909. [PubMed: 17504862]
20. Park JW, Kim JH, Kim SK, Kang W, Park KW, Choi JI, et al. A Prospective Evaluation of ^{18}F-FDG and ^{11}C-Acetate PET/CT for Detection of Primary and Metastatic Hepatocellular Carcinoma. J Nucl Med. 2008; 49:1912–1921. [PubMed: 18997056]
21. Hwang KH, Choi DJ, Lee SY, Lee MK, Choe W. Evaluation of patients with hepatocellular carcinomas using [^{11}C]acetate and [^{18}F]FDG PET/CT: A preliminary study. Appl Radiat Isot. 2009; 67:1195–1198. [PubMed: 19342249]
22. Talbot JN, Gutman F, Fartoux L, Grange JD, Ganne N, Kerrou K, et al. PET/CT in patients with hepatocellular carcinoma using [^{18}F]fluorocholine: preliminary comparison with [^{18}F]FDG PET/CT. Eur J Nucl Med Mol Imaging. 2006; 33:1285–1289. [PubMed: 16802155]
23. Yamamoto Y, Nishiyama Y, Kameyama R, Okano K, Kashiwagi H, Deguchi A, et al. Detection of hepatocellular carcinoma using ^{11}C-choline PET: comparison with ^{18}F-FDG PET. J Nucl Med. 2008; 49:1245–1248. [PubMed: 18632827]
24. Eckel F, Herrmann K, Schmidt S, Hillerer C, Wieder HA, Krause BJ, et al. Imaging of proliferation in hepatocellular carcinoma with the in vivo marker ^{18}F-fluorothymidine. J Nucl Med. 2009; 50:1441–1447. [PubMed: 19690030]
25. Ishiwata K, Yamaguchi K, Kameyama M, Fukuda H, Tada M, Matsuzawa T, et al. 2-Deoxy-2-[^{18}F]fluoro-D-galactose as an in vivo tracer for imaging galactose metabolism in tumours with positron emission tomography. Int J Rad Appl Instrum B. 1989; 16:247–254. [PubMed: 2785512]
26. Paul R, Aho K, Bergman J, Haaparanta M, Kulmala J, Reissell A, et al. Imaging of Rats with mammary cancer with two 2-Deoxy-2-[^{18}F]fluoro-D-hexoses. Int J Rad Appl Instrum B. 1989; 16:449–453. [PubMed: 2509402]
27. Ishiwata K, Takahashi T, Iwata R, Tomura M, Tada M, Itoh J, et al. Tumour diagnosis by PET: Potential of seven tracers examined in five experimental tumours including an artificial metastasis model. Int J Rad Appl Instrum B. 1992; 19:611–618. [PubMed: 1387872]
28. Fukuda H, Takashi J, Fujiwara T, Yamaguchi K, Abe Y, Kubota K, et al. High accumulation of 2-deoxy-fluorine-18-fluoro-D-galactose by well-differentiated hepatomas of mice and rats. J Nucl Med. 1993; 34:780–786. [PubMed: 8478711]
29. Sørensen M, Munk OL, Mortensen FV, Olsen AaK, Bender D, Bass L, et al. Hepatic uptake and metabolism of galactose can be quantified in vivo by 2-[^{18}F]Fluoro-2-deoxy-galactose Positron Emission Tomography. Am J Physiol Gastrointest Liver Physiol. 2008; 296:G27–G36.
30. Sørensen M. Determination of hepatic galactose elimination capacity using 2-[^{18}F]fluoro-2-deoxy-D-galactose PET/CT. Reproducibility of the method and metabolic heterogeneity in a normal pig liver model. Scand J Gastroenterol. 2011; 46:98–103. [PubMed: 20695723]

31. Frisch K, Bender D, Hansen SB, Keiding S, Sørensen M. Nucleophilic radiosynthesis of 2-[^{18}F]fluoro-2-deoxy-d-galactose from Talose triflate and biodistribution in a porcine model. Nucl Med Biol. 2011 in press.

32. Pugh RN, Murray-Lyon IM, Dawson JL, Pietroni MC, Williams R. Transection of the oesophagus for bleeding oesophageal varices. Br J Surg. 1973; 60:646–649. [PubMed: 4541913]

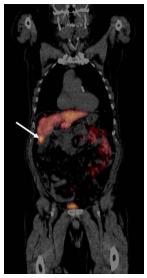

Fig 1.

PET/CT image of an FDGal positive HCC lesion (arrow) in a cirrhotic liver (ID33; coronal view). The diagnosis was based on plasma AFP (1076 ng/ml) and multi-phase ceCT according to internationally approved guidelines [5, 6]. The aetiology was alcoholic cirrhosis.

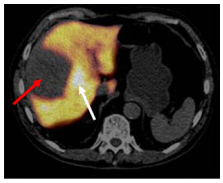

Fig. 2.

FDGal PET/CT image (a) and ceCT image in arterial phase (b) of a large necrotic HCC (white arrows) with adjacent viable tumour tissue (red arrows) (ID22, transaxial view). The patient did not have cirrhosis and the aetiology was unknown. Plasma AFP was 3047 ng/ml and the multi-phase ceCT typical for HCC [5, 6].

Fig. 3.

Example of a large HCC with low metabolic activity seen as an area with low FDGal uptake on the FDGal PET/CT image (a), atypical low contrast-enhancement in the arterial phase of multi-phase ceCT, and typical washout pattern in the late venous phase on ceCT(c) (ID12, transaxial view). A biopsy showed HCC (medium differentiated). The aetiology was alcoholic cirrhosis and plasma AFP was 11 ng/ml.

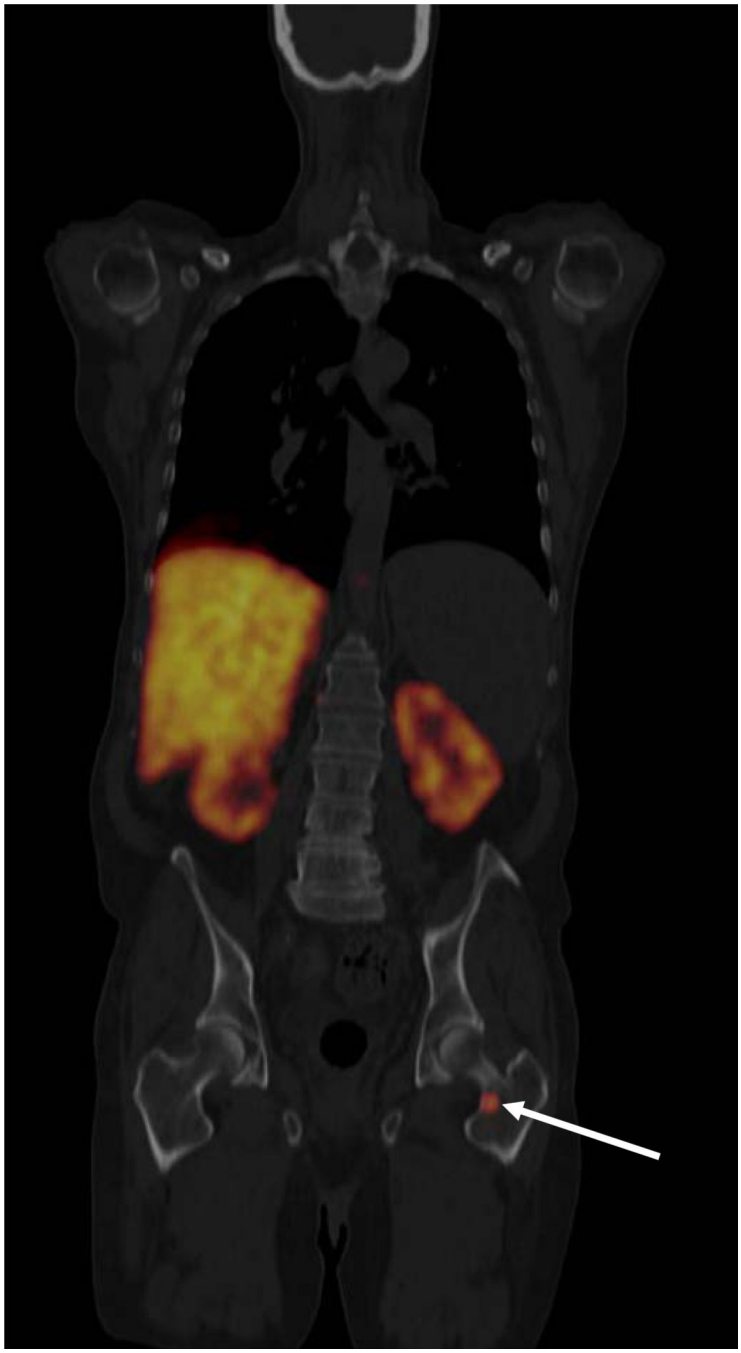

Fig. 4.

FDGal PET/CT image showing a metastasis in the neck of the left femur bone (ID27, coronal view). The liver is large and cirrhotic with no visible tumours in this plane. Radioactivity in the kidneys is physiological due to excretion of FDGal in the urine. The patient had cirrhosis (hepatitis C) and HCC was verified by biopsy. AFP was 13 ng/ml.

Table 1

Patient characteristics

	All patients included (*n*=39)	Patients with HCC included before treatment	Patients with HCC included after treatment	Patients with the final diagnosis not being HCC
Female/Male	16/23	7/16	4/5	5/2
Age, years	61 [40–86]	64 [40–86]	60 [51–83]	50 [43–57]
Child-Pugh Class A/B/C[a]	19/9/4	12/5/3	3/1/1	4/3/0
Cirrhosis/non-cirrhosis	31/8	19/4	5/4	7/0
HCV/HBV/alcohol/PBC/autoimmune/other[b]	10/1/12/3/3/10	6/1/8/3/1/4	1/0/3/0/0/5	3/0/1/0/2/1
AFP, ng/ml	26 [1–285,199]	98 [3–285,199]	4 [1–90,748]	4 [1–41]
Biopsy, yes/no	29/10[c]	16/7[c]	9/0	4/3

Qualitative variables are given as total and continuous variables are given as median [range]. HCV, hepatitis C virus; HBV, hepatitis B virus; PBC, primary biliary cirrhosis; AFP, alpha-fetoprotein.

[a] Seven patients without liver disease were not classified according to the Child-Pugh classification.

[b] Other causes included cryptogenic cirrhosis (*n*=6), steatosis (*n*=1), McKusick Kaufmann Syndrome (*n*=1), and unknown (*n*=2).

[c] One patient (ID32) had a false-negative biopsy.

Table 2

Patients with HCC included before treatment

Patient ID	Age, years	Sex	Interpretation of FDGal PET images	Interpretation of ceCT images	Other imaging modalities or follow-up	T/B-ratio on FDGal PET
1	71	F	Multinodular disease	Multinodular disease		1.6
3	61	M	Multinodular disease	Multinodular disease		1.6
4	52	M	Multinodular disease	Multinodular disease		2.0
5	73	M	Multinodular disease	Multinodular disease		1.7
6	48	M	Several suspicious nodules	Four nodules	Rapid progression to multinodular	1.3
7	70	F	Multinodular disease	Multinodular disease		1.4
8	50	M	Two lesions	Several dense areas, one suspicious	US: two lesions	Both 1.2
9	71	M	One lesion in right lobe, one suspicious in left lobe	One lesion in left liver lobe	US: one lesion	Both 1.4
10	40	F	Multinodular disease	Multinodular disease		1.8
12	71	M	Necrotic tumour	Necrotic/hypoperfused		0.8
15	69	F	Necrotic tumour	Necrotic tumour		0.7
17	64	M	Multinodular disease	Multinodular disease	US: one minor lesion	1.4 – 1.8
19	64	M	Multinodular disease with necrotic areas	Multinodular disease with necrotic areas		1.3 (viable) 0.4 (necrosis)
20	49	M	Multinodular disease	One small suspicious lesion	US: no lesions Died 7 weeks later (multinodular HCC)	1.4
21	51	M	Large necrotic tumour	Large necrotic tumour	US: two lesions	0.3
22	77	M	Large tumour with central necrosis	Lager tumour with central necrosis		1.5 (viable) 0.3 (necrosis)
24	86	F	Two lesions	One lesion	Progression in PET positive areas	1.7; 1.3
27	59	M	Three distinct lesions	No lesions	MRI: one lesion, biopsy positive Follow-up: several lesions on US	1.4 – 1.8
28	73	F	No lesions	One lesion	US: one lesion, biopsy-positive	n.d.
32	61	M	Multinodular disease	Multinodular disease	US: Multinodular	1.3 – 2.8
33	63	M	Three lesions	Three lesions	US: two lesions	1.6 – 1.9
35	78	F	Large necrotic tumour	Large necrotic tumour		0.6
36	85	M	Large necrotic tumour	Large necrotic tumour		0.2

FDGal, 2-[^{18}F]fluoro-2-deoxy-D-galactose; ceCT, contrast-enhanced CT; T/B-ratio, tumour-to-background ratio; F, female; M, male; US, ultrasound sonography; MRI, magnetic resonance imaging; n.d., not determined.

Table 3

Patients with HCC included after treatment

Patient ID	Age, years	Sex	Type and time of treatment	Interpretation of FDGal PET images	Interpretation of ceCT images	Other imaging modalities or follow-up	T/B-ratio on FDGal PET
2	57	M	TACE one month before PET	Multinodular disease No necrosis	Multinodular disease No necrosis		2.6
13	83	M	TACE 2 months before PET; previously 4xRFA	Response to treatment	Response to treatment		0.2 – 0.7
14	51	F	RFA and TACE several times before, SBRT	Necrosis, no visible tumour	Necrosis, no visible tumour		0.2
18	54	F	RFA 6 months and TACE 3.5 months before PET	Residual tumour with areas of necrosis	Residual tumour with areas of necrosis		0.1 (necrosis) 1.4 (viable)
23	62	M	TACE of tumour mass in left liver lobe one week before PET	Treatment response in left liver lobe, two lesions in right liver lobe	Treatment response in left liver lobe, two lesions in right liver lobe		0.1 (necrosis) 1.3 (viable)
29	60	M	RFA two years before PET	RFA-necrosis Small lesion in right liver lobe	RFA-necrosis Small lesion in right liver lobe		0.2 (necrosis) 1.2 (viable)
34	62	F	Hepatic resection 6 years before PET	No suspicious lesions	- - -	MRI: tumour in left kidney Biopsy: Renal cell carcinoma	- - -
37	57	M	RFA 6 days before PET	No viable tumour	No viable tumour		0.3
39	72	F	RFA 6 months and TACE one month before PET	Treatment response Two lesions in right liver lobe	Several lesions (pre-treatment)	TACE was repeated	0.4 (necrosis) 1.3 (viable)

FDGal, 2-[^{18}F]fluoro-2-deoxy-D-galactose; ceCT, contrast-enhanced CT; T/B-ratio, tumour-to-background ratio; F, female; M, male; TACE, transarterial chemoembolization; RFA, radiofrequency ablation; SBRT, stereotactic body radiation therapy. ID34 was allergic to contrast and a ceCT was not performed.

Table 4

Patients with the final diagnosis not being HCC

Patient ID	Age, years	Sex	Interpretation of FDGal PET images	Interpretation of ceCT images	Final diagnosis
11	51	F	No lesions	Three lesions	No cancer
16	55	F	No lesions	One suspicious lesion	No cancer
25	54	M	No lesions	One suspicious lesion	Pancreatic cancer
26	57	M	No lesions	One suspicious lesion	No cancer
31	48	F	No lesions	US: lymph node in porta hepatis	No cancer
38	45	F	No lesions	One suspicious lesion US: one suspicious lesion	Haemangioma
40	43	F	No lesions	ceCT+MRI+US: one suspicious lesion	Adenoma

FDGal, 2-[^{18}F]fluoro-2-deoxy-D-galactose; ceCT, contrast-enhanced CT; F, female; M, male; US, ultrasound sonography; MRI, magnetic resonance imaging.

Table 5

Patients with extra-hepatic metastases

Patient ID	Age, years	Sex	Location of extra-hepatic HCC	T/B-ratio on FDGal PET
07	70	F	Lymph node in right axilla	11
13	83	M	Right lung	17.5
14	51	F	Left scapula Left maxillary sinus	17 11
15	69	F	Lymph node in commom hepato-biliary ligament	2.4
21	51	M	Left lung	1.3
23	62	M	Two in right lung	Both 4.5
27	59	M	Left femoral collar	27
35	78	F	Right lung	12
39	72	F	Lymph node right side of neck Right side of the hyoid bone	4.3 4.3

F, female; M, male; FDGal, 2-[^{18}F]fluoro-2-deoxy-D-galactose; T/B-ratio, tumour-to-background ratio when compared to contra-lateral side.